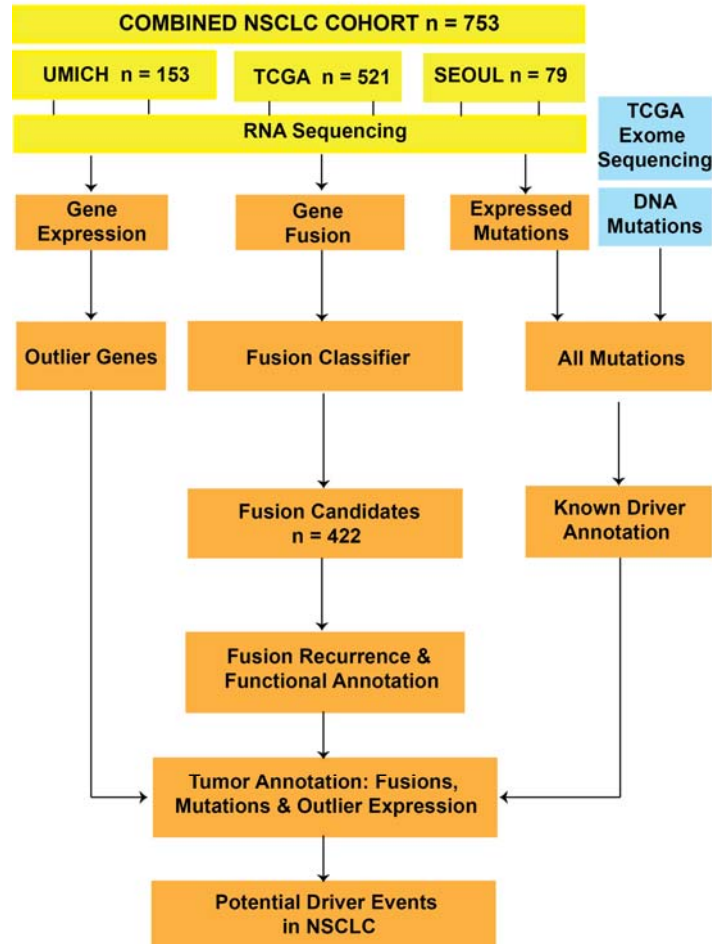
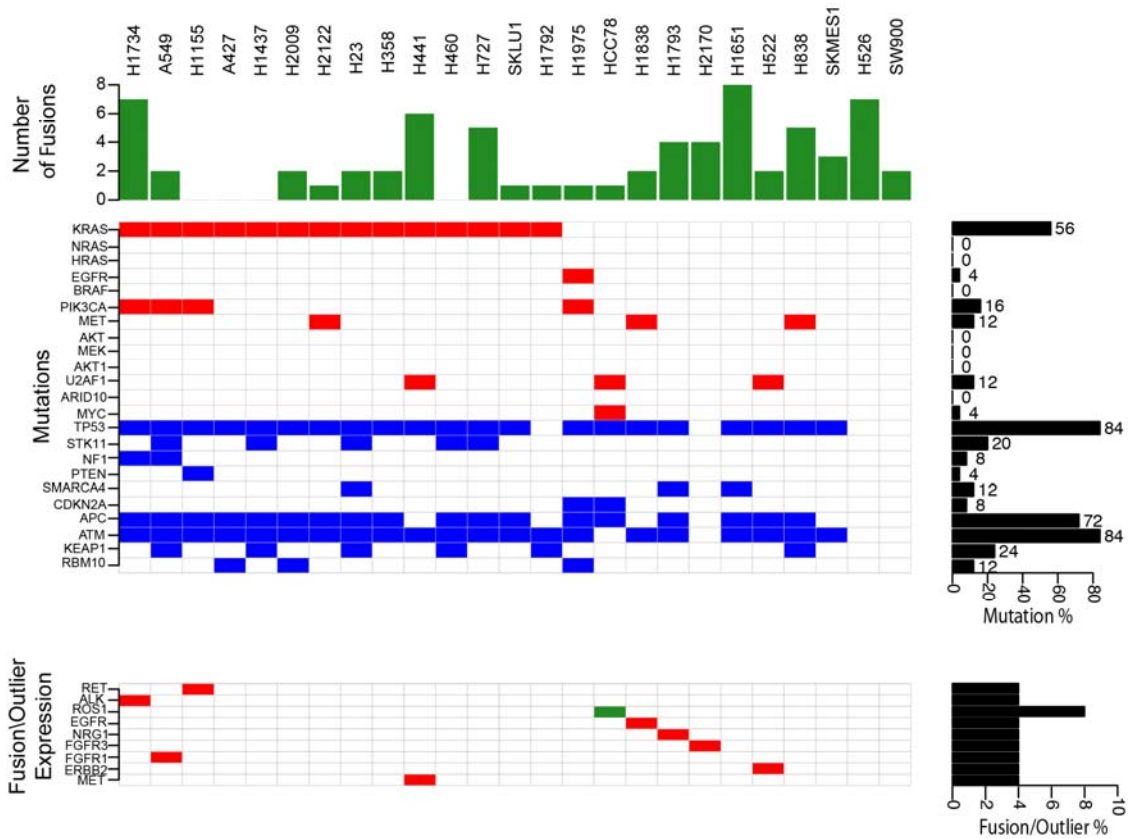


Supplementary Figure 1



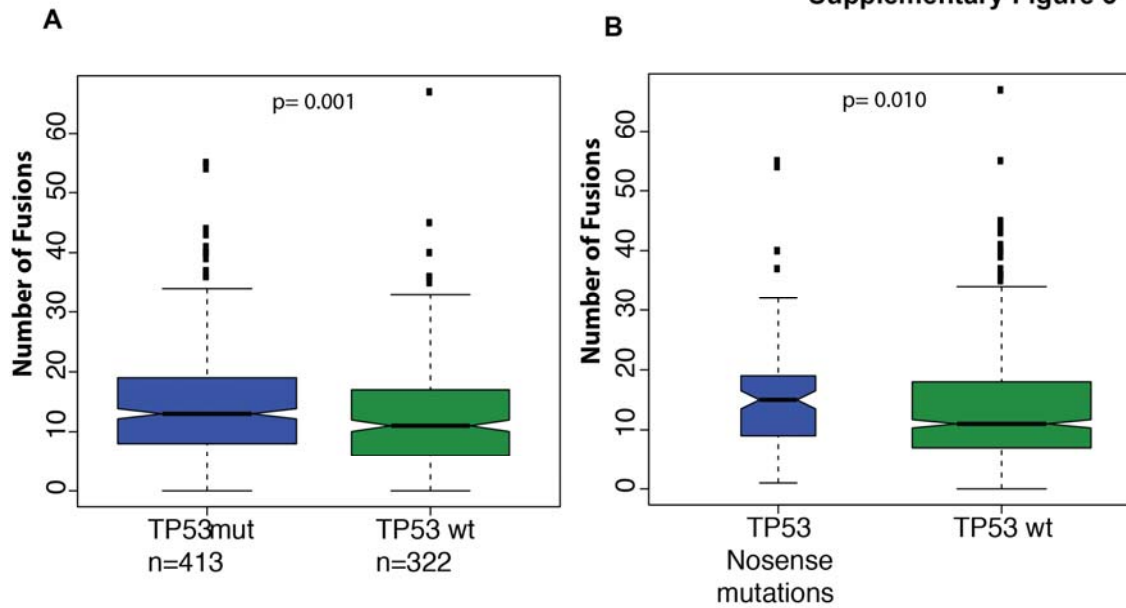
Supplementary Figure 1. Schematic diagram of the data generation and analysis workflow of lung cancer RNASeq data. A total of 753 lung cancer samples that include 728 clinical specimens and 24 cell lines, representing 451 LUAD and 251 LUSC, 11 LACC and 9 LCLC were interrogated for gene fusions and somatic mutations. The cohort was assembled combining 133 University of Michigan samples (UMICH), 79 Seoul National University samples (SEOUL), and 521 Cancer Genome Atlas samples (TCGA). The RNASeq data was mapped to human RefSeq Hg19 using TopHat2. Fusion calls were made with TopHat-Fusion (THF). In all cases fusions present in normal samples were considered false positives and filtered out. We developed and applied a fusion classifier that retained 422 gene fusions for further downstream analysis. The 422 fusions were classified into recurrent (>2 samples) and private fusions and further divided into inter chromosomal, intra chromosomal or fusions resulting from potential tandem duplication events. In addition samples were annotated for outlier expressions and somatic/COSMIC mutations in well-known lung oncogene drivers and tumor suppressors. Finally, both LUAD and LUSC cohorts were divided into either samples harboring oncogene driving mutations or samples without known driver genes.

Supplementary Figure 2



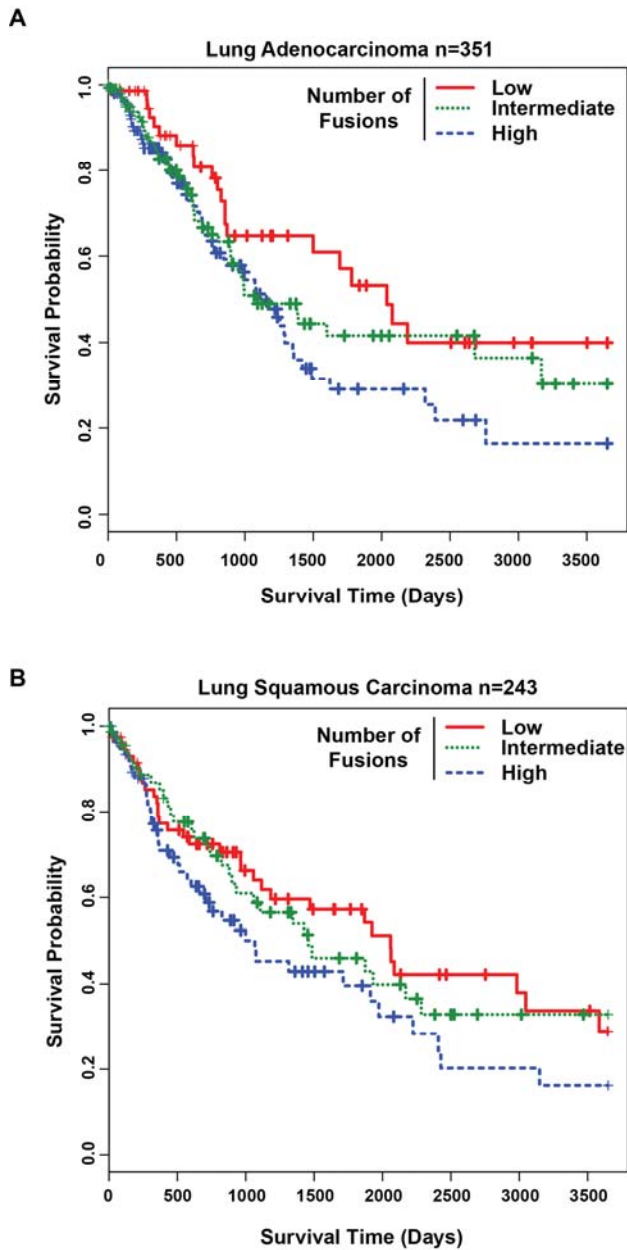
Supplementary Figure 2: Gene Fusions, Mutations and outliers in Lung Cancer Cell Lines. Histograms represent the number of prioritized fusions identified in each cell line sample. **Central Panel:** Heatmap denotes the presence or absence of activating mutations in known oncogenes (red) and deleterious mutations in tumor suppressors (blue). Samples are presented in columns and genes are in rows. **Right Middle Panel:** Bar plot summarizes the number of samples harboring activating or deleterious mutations for each gene. **Bottom Panel:** Heatmap displays samples harboring known gene fusions (green) involving receptor kinase genes. Samples in red indicate outlier expression pattern observed in the respective genes. The ordering of samples in center panels was dictated by mutation status in *KRAS*, *NRAS*, *HRAS*, *EGFR*, *BRAF*, *PIK3CA*, and *TP53* genes in that order. The bottom right histogram outlier percentage expression in the cell line panel. Data from the small cell lung cancer cell line H526 is shown alongside the NSCLC cell lines for comparison.

Supplementary Figure 3



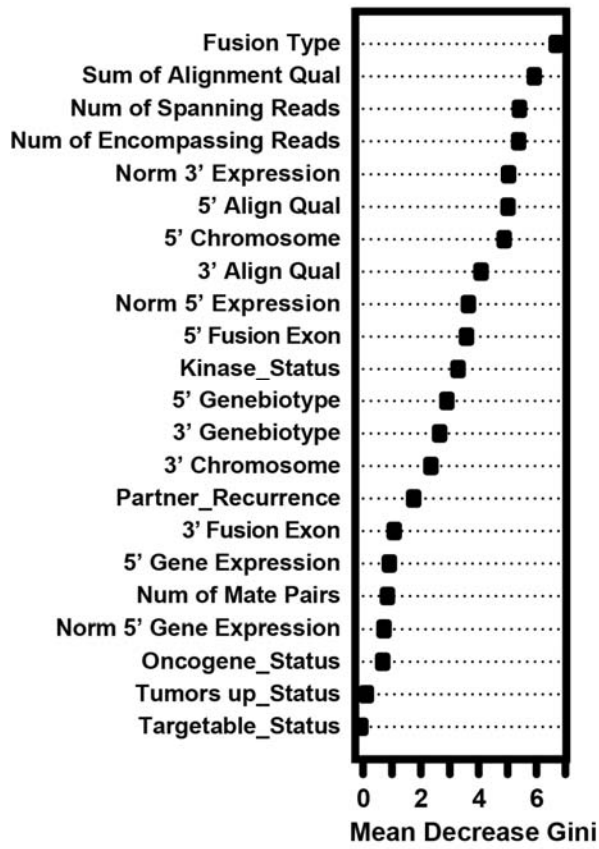
Supplementary Figure 3: Comparison between the Number of Fusions and *TP53* Mutation Status. **A.** Box plot representation of number of fusions in *TP53* wildtype vs all *TP53* mutated samples **B.** Box plot representation of number of fusions in *TP53* wildtype vs *TP53* nonsense mutations containing samples.

Supplementary Figure 4



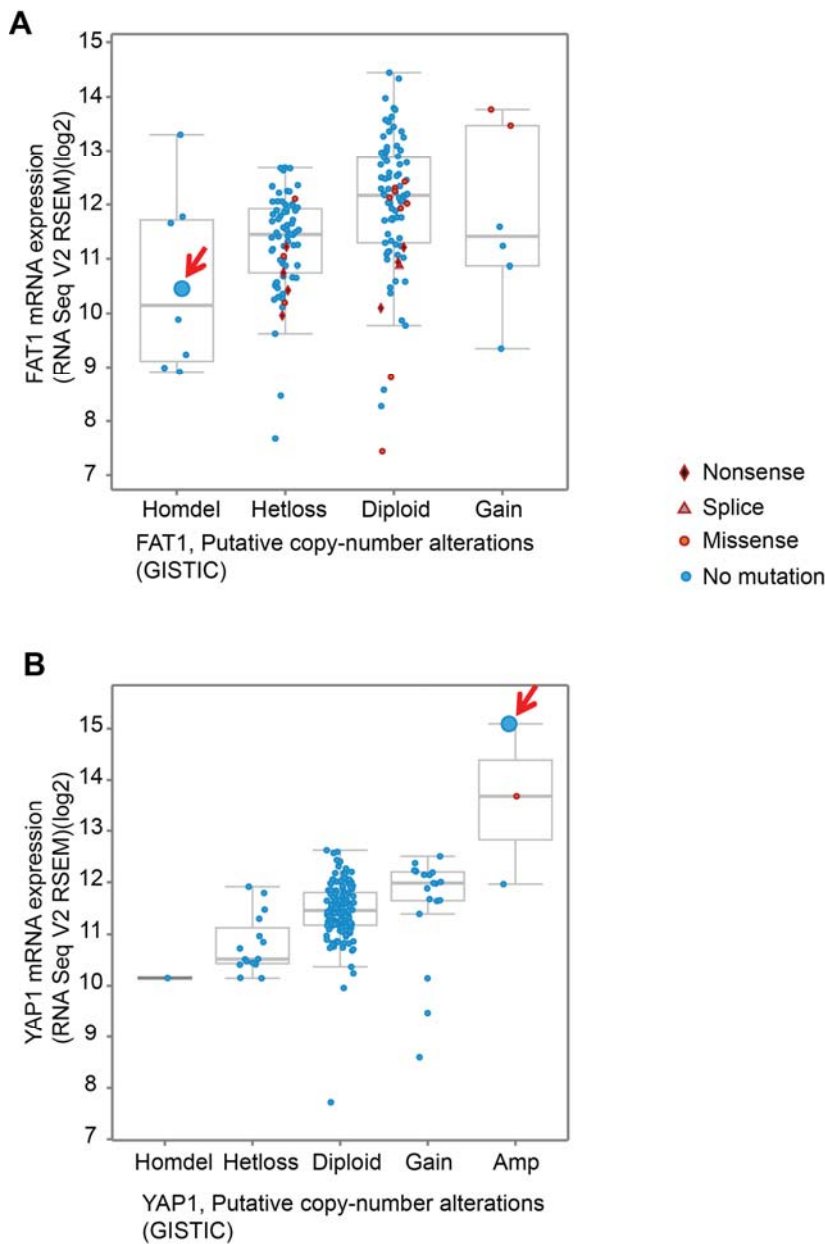
Supplementary Figure 4: Gene fusion frequency is a prognostic indicator in both LUAD and LUSC. **A.** Kaplan-Meier survival curve for LUAD samples (n=351) with low (0-6) (n=55), intermediate (7-12) (n=185), or high (≥ 13) (n=111) number of fusions (Likelihood ratio test $P=0.07562$). Samples with high number of fusions have worst prognosis (Cox survival analysis $P=0.0291$). **B.** Kaplan-Meier survival plot for LUSC samples (n=243) with low (0-11) (n=62), intermediate (12-18) (n=112) and high (≥ 19) (n=69) number of fusions (Likelihood ratio test $P=0.1685$). Samples with high number of fusions have worst prognosis (Cox survival analysis $P=0.0717$).

Supplementary Figure 5



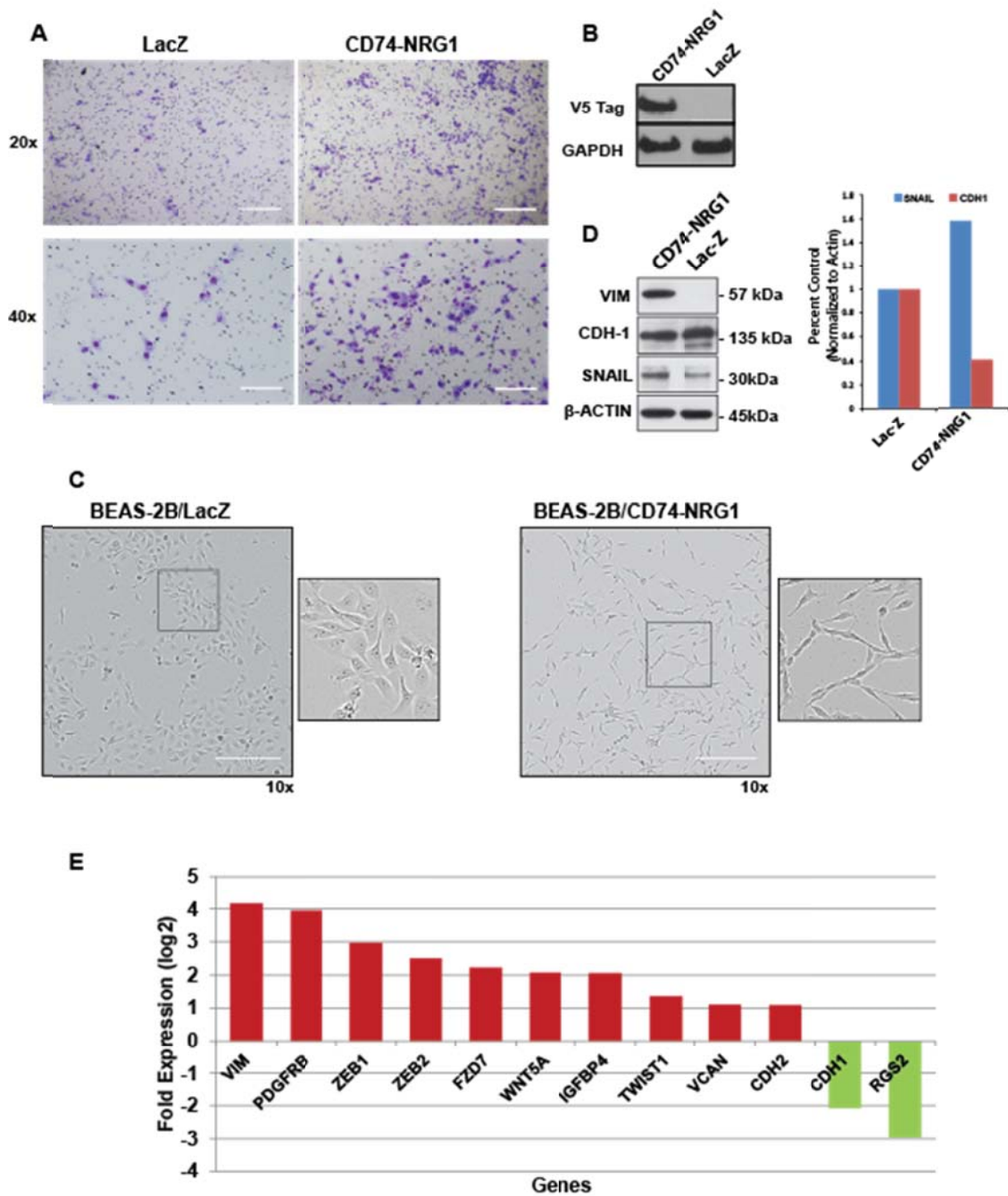
Supplementary Figure 5: Features Used by the Fusion Classifier. Importance of fusion classifier features in decreasing order (mean decrease GINI).

Supplementary Figure 6



Supplementary Figure 6. Integrative analysis of Hippo pathway gene aberrations in the fusion index cases. Box plot representation of mutation and copy number status along with mRNA expression values for the indicated Hippo pathway genes were generated using the analysis tool embedded in cbiportal (<http://www.cbiportal.org>) (A) *FAT1*(TCGA-43-3920) and (B) *YAP1* (TCGA-22-1016) aberration status in TCGA LUSC cohort (n=271) and in the corresponding index cases (sample-IDs in parenthesis, represented by large blue dots indicated with red arrow in the box plots). Red diamonds-Nonsense mutations; Red triangle-Splice mutation; Red dot: Missense mutation; Small blue dots- no mutation.

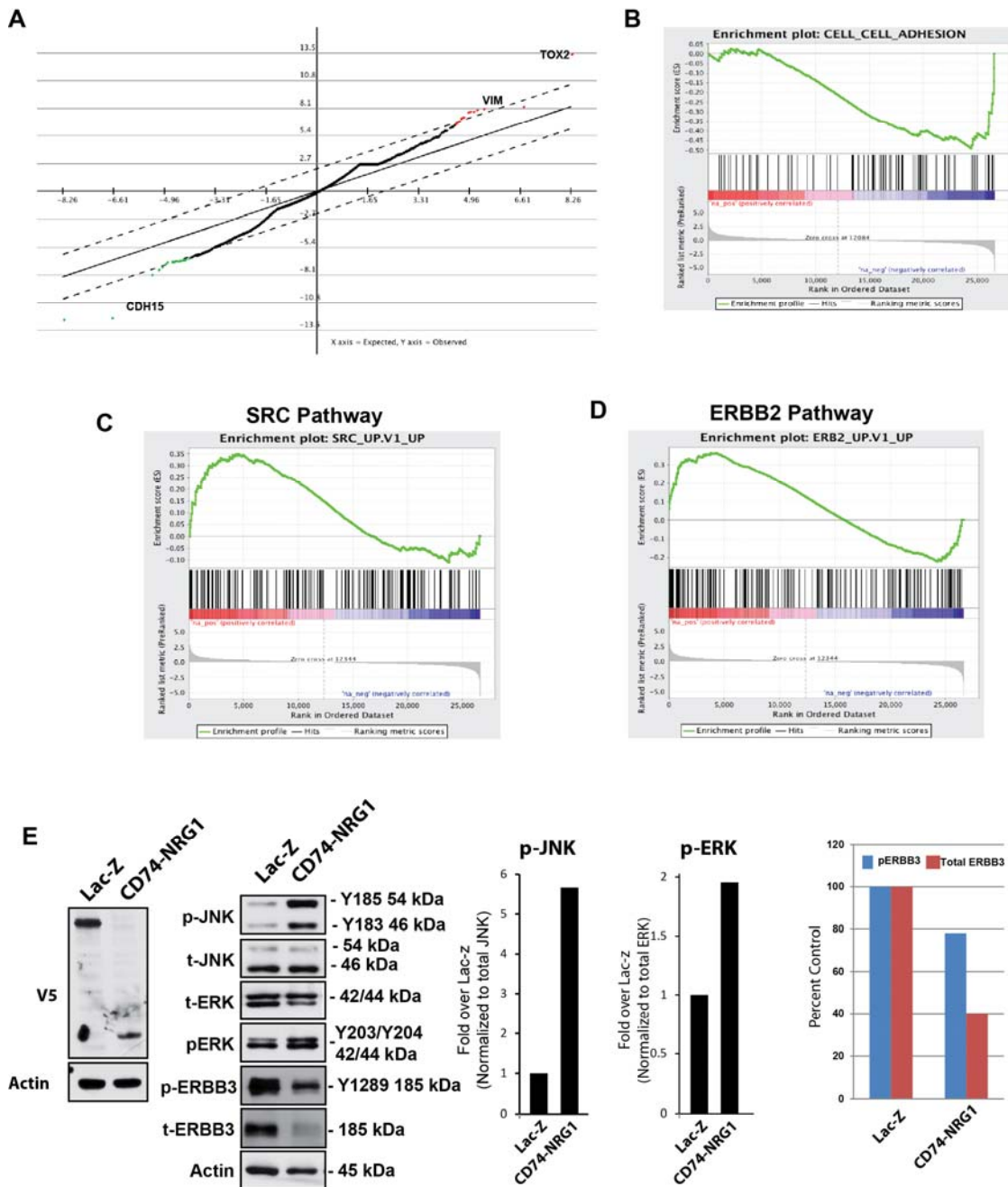
Supplementary Figure 7



Supplementary Figure 7: Functional Characterization of NRG1 fusion. **A.** Representative pictures of cells migrating to the basal side of the Boyden chamber membrane after Diff-Quick staining with an Olympus microscope at 20x magnification. White scale bar 100um **B.** Western blot analysis with V5 epitope tag to monitor CD74-NRG1 fusion and control GAPDH protein expression in BEAS-2B stable cells. Blot images have been cropped for presentation; full size images are presented in Supplementary Figure 9. **C.** Representative pictures of BEAS-2B cells expressing the

CD74-NRG1 fusion or Lac-Z. Cells expressing the CD74-NRG1 fusion appeared smaller and more fusiform as compared to Lac-Z, suggesting that they acquired a more mesenchymal phenotype. Boxed regions are enlarged sections on the right. White scale bar 200um **D.** Western blot analysis of E-cadherin (CDH-1) and Vimentin protein expression in transfected BEAS-2B cells. CD71-NRG1 transfected cells, showed a modest decrease in CDH-1 and a significant increase of Vimentin protein expression. Western Blot images have been cropped for presentation; full size images are presented in Supplementary Figure 9. **E.** Gene expression pattern for various epithelial mesenchymal transition markers from microarray data (log₂ ratios). Western Blot images have been cropped for presentation; Full western blot images are presented in **Supplementary Fig 9.**

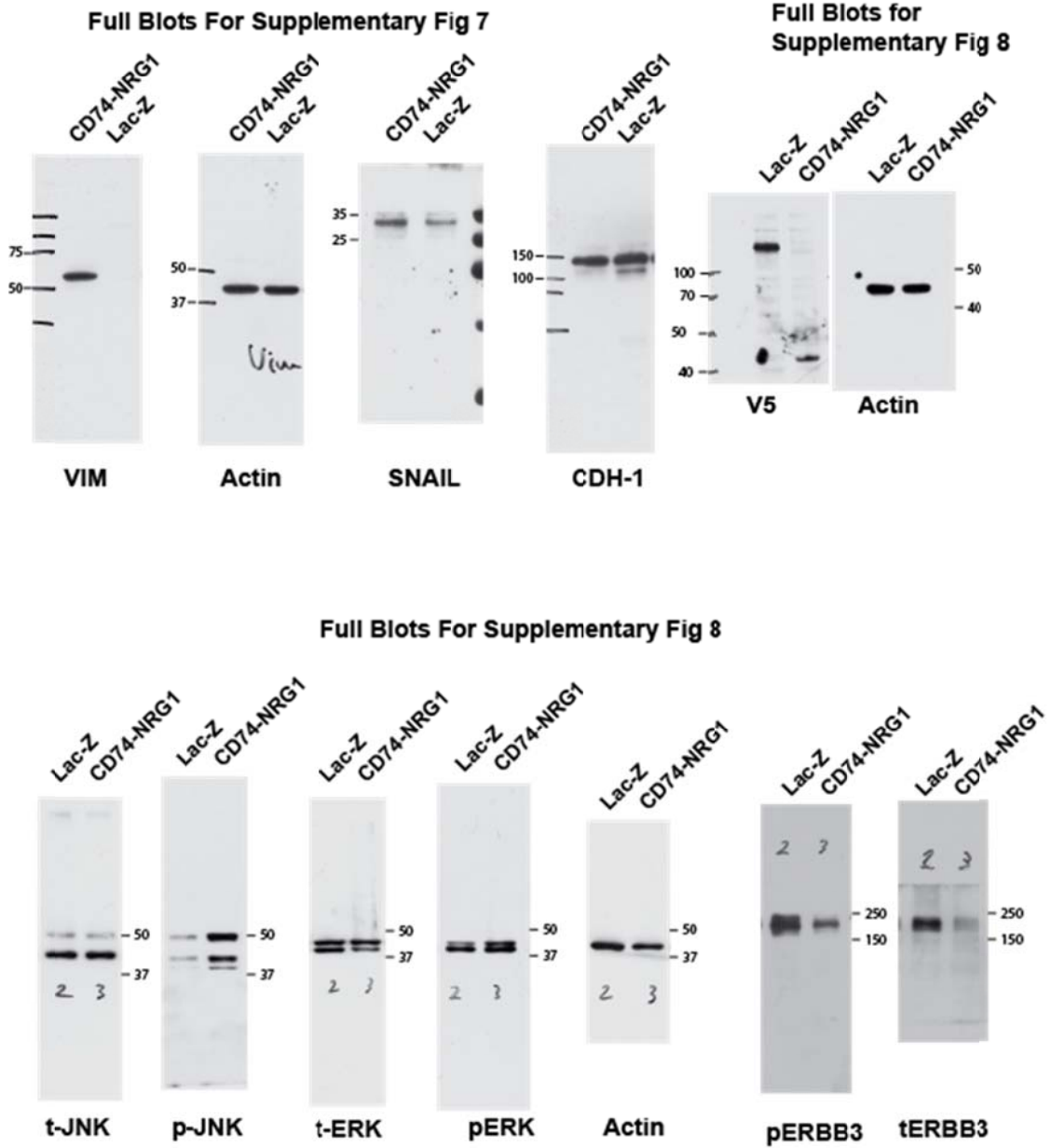
Supplementary Figure 8



Supplementary Figure 8: Gene Expression Analysis of *CD74-NRG1* Expressing Cells
A. Differentially expressed genes identified by one class Significance Analysis of Microarrays (SAM). SAM-Plot represents the 35 genes with significant differential expression at 10% FDR (False Discovery Rate). **B, C and D.** Gene set enrichment analysis based on differentially-expressed genes among BEAS-2B cells transfected with the *CD74-NRG1* fusion or Lac-Z. Significant up-regulation of cell-cell adhesion, SRC and ERBB2 pathways was observed in CD74-NRG1 cells respectively. **E.** Western blot

analysis to examine the levels of LacZ, CD74-NRG1, total and phosphorylated ERBB3, ERK and JNK1 proteins. Both lacZ and CD74-NRG1 fusion protein contains V5 epitope tag and their expression was evaluated by V5 antibody immunoblot. Barplots represent densitometric quantitation of phospho ERK, phospho JNK and ERBB3 protein levels. Western Blot images have been cropped for presentation; Full western blot images are presented in **Supplementary Fig 9**.

Supplementary Figure 9:



Supplementary Figure 9: Representative full Western blot images presented in Supplementary Figures 7 and 8.

Supplementary Table 1: Summary of Clinicopathological Characteristics for all Patients in the Combined Cohort.

SAMPLES							
	LUAD	LUSC	LUCL	Normal	LCLC	LACC	TOTAL
UMICH	67	36	24	6	9	11	153
SEOUL	79	0	0	0	0	0	79
TCGA	305	216	0	0	0	0	521
TOTAL	451	251	24	6	9	11	753
GENDER							
	MALE	FEMALE					
UMICH	64	58					
SEOUL	48	31					
TCGA	298	223					
TOTAL	410	312					
FOLLOW UP TIME							
	MIN	MEDIAN	MAX	AVAILABLE			
UMICH	0.26	4.64	17.37	111			
SEOUL	NA	NA	NA	0			
TCGA	0	0.92	18.66	436			
TUMOR STAGE							
	STAGE I	STAGE II	STAGE III	STAGE IV			
UMICH	67	23	24	0			
SEOUL	NA	NA	NA	NA			
TCGA	250	112	101	19			
SMOKING STATUS							
	NEVER SMOKER	LIGHT SMOKER	HEAVY SMOKER				
UMICH	0	13	82				
SEOUL	NA	NA	NA				
TCGA	4	72	309				

Supplementary Table 2: Non Synonymous Mutations in Lung Adenoid Cystic Carcinoma and Large Cell Lung Cancer Samples.

S.No	Sample	Cancer Type	Cosmic Mutations													
			Region	KRAS	NRAS	HRAS	BRAF	KIT	MET	TP53	IDH1	GNAS	ATM	NF1		
1	pt_lung_ACC_07-I-5699	Lung Adenoid Cystic Carcinoma	Exonic	G12C												
2	pt_lung_ACC_09-D-5737	Lung Adenoid Cystic Carcinoma	Exonic	G12V												
3	pt_lung_ACC_12-I-2857	Lung Adenoid Cystic Carcinoma	Exonic	G12D												
4	pt_lung_ACC_12-I-4664	Lung Adenoid Cystic Carcinoma	Exonic	Q61H										R186H, R187H		
5	pt_lung_ACC_09-I-7040	Lung Adenoid Cystic Carcinoma	Exonic	G13C					M541L		R141L					
6	pt_lung_ACC_12-I-3344	Pulmonary Met*	Exonic		Q61R				M541L	T992I,T1010I	R141C					
7	pt_lung_ACC_10-D-6174	Lung Adenoid Cystic Carcinoma	Exonic			Q61L										
8	pt_lung_ACC_09-I-5904	Lung Adenoid Cystic Carcinoma	Exonic					V600E								
9	pt_lung_ACC_11-T-230	Lung Adenoid Cystic Carcinoma	Exonic									V178I				
10	pt_lung_ACC_11-I-8842	Lung Adenoid Cystic Carcinoma	No nominations													
11	pt_lung_ACC_12-I-318	Lung Adenoid Cystic Carcinoma	No nominations													
12	pt_lung_LC14	Large Cell Lung Cancer	No nominations													
13	pt_lung_LC4	Large Cell Lung Cancer	No nominations													
14	pt_lung_LC1	Large Cell Lung Cancer	Exonic								C176S					
15	pt_lung_L63	Large Cell Lung Cancer	No nominations													
16	pt_lung_LC3	Large Cell Lung Cancer	Exonic	R151G							F113S		P129L	K2530E, S85P		
17	pt_lung_LC13	Large Cell Lung Cancer	No nominations													
18	pt_lung_LC2	Large Cell Lung Cancer	Exonic	G12V												
19	pt_lung_LC8	Large Cell Lung Cancer	Exonic	R151G							E166X					Y1254H
20	pt_lung_LC9	Large Cell Lung Cancer	Exonic													E149K

* from Colon Adenocarcinoma

Supplementary Table 3: Comparison of the number of fusions among different tumor stages in LUAD and LUSC.

LUAD	Stage I	Stage II	Stage III	Stage IV
Stage I		0.294	0.783	0.147
Stage II			0.219	0.049
Stage III				0.201

LUSC	Stage I	Stage II	Stage III	Stage IV
Stage I		0.014	0.726	0.093
Stage II			0.060	0.020
Stage III				0.075

Supplementary Table 4: Univariate Cox regression for overall survival according to clinical variables (n = 621).

	Overall Survival		
	HR	95% CI	p-value
Age, continuous	1.03	1.01 – 1.04	< 0.001
Sex			
Female	1	--	
Male	1.33	1.02 – 1.74	0.037
Stage, continuous	1.55	1.35 – 1.76	< 0.001
Smoking status			
Non-smoker	1	--	
Smoker (<35 pack-year)	1.31	0.52 – 3.30	0.565
Smoker (≥35 pack-year)	1.49	0.61 – 3.67	0.378
Histology			
Adenocarcinoma	1	--	
Squamous cell carcinoma	0.99	0.76 – 1.29	0.989
TP53 status			
Wild-type	1	--	
Mutant	0.94	0.66 – 1.33	0.717
KRAS status			
Wild-type	1	--	
Mutant	0.94	0.66 – 1.33	0.717
EGFR status			
Wild-type	1	--	
Mutant	1.01	0.77 – 1.33	0.924

Supplementary Table 5: Multivariate Cox Regression for Overall Survival According to Number of Fusions in 621 NSCLC Patients Adjusted by Age, Gender and Stage.

Covariates in the Model		Hazard Ratio	95% Confidence Intervals	p-value
Age, continuous		1.04	1.02 – 1.05	<0.001
Gender	Female	1	–	
	Male	1.17	0.89 – 1.56	0.233
Stage, continuous		1.63	1.42 – 1.87	<0.001
Number of Fusions	Low	1		
	Intermediate	1.13	0.79 – 1.61	0.484
	High	1.58	1.15 – 2.18	0.004

Supplementary Table 6: Multivariate Cox regression for overall survival according to number of fusions in 621 NSCLC patients adjusted by age, gender, stage and mutational status.

Covariates in the Model		Hazard Ratio	95% Confidence Intervals	p-value
Age, continuous		1.04	1.02 – 1.06	<0.001
Gender	Female	1	–	
	Male	1.22	0.96 – 1.85	0.082
Stage, continuous		1.6	1.37 – 1.87	<0.001
Smoking status	Never-smoker	1		
	Smoker (<35py)	1.03	0.39 – 2.67	0.956
	Smoker (≥35py)	1.04	0.40 – 2.66	0.938
Histology	LUAC	1	–	
	LUSC	0.9	0.63 – 1.27	0.524
Number of fusions	Low	1		
	Intermediate	1.34	0.91 – 2.08	0.125
	High	1.75	1.18 – 2.59	0.005
KRAS status	WT	1	–	
	mutant	1.17	0.76– 1.81	0.471
EGFR status	WT	1	–	
	mutant	1.32	0.87 – 2.01	0.183
TP53 status	WT	1	–	
	mutant	1.2	0.86 – 1.69	0.385

Supplementary Table 7: NF1 Aberrations in NSCLC.

S.No	Sample_ID	Cohort	Fusion partners	NF1_Aberration	NF1_Mutation	Other_Mutations	Fusion ORF
1	TCGA-43-6413	TCGA	GOSR1-NF1	Fusion			No
2	TCGA-69-7764	TCGA	NLK-NF1	Fusion	p.T2335P		No
3	pt_lung_LS2	UMICH	NF1-DRG2_AS	Fusion			No
3	pt_lung_LS2	UMICH	NF1-MYO15A_AS	Fusion			No
4	TCGA-44-5644	TCGA	NF1-PSMD11	Fusion	p.H553Y		Yes
S.No	Patient_UID	Cohort	Gene	NF1_Aberration	NF1_mutation	Other_Mutations	
5	2c8877f9-ee7f-4216-97ad-d2939a13daa4	TCGA	NF1	Mutation	p.C904*	PIK3CA p.E545K;	
6	3c4ff061-d214-4d1c-8d2e-3034f207c252	TCGA	NF1	Mutation	p.E126*	cMET exon skipping 14	
7	6bffe800-ec2b-4638-9333-97fe85dcd91c	TCGA	NF1	Mutation	p.E1947*&p.W1831fs		
8	b4ff0f49-b787-48ec-91cc-ee26786ff1bf	TCGA	NF1	Mutation	p.E2231*		
9	pt_lung_C115	UMICH	NF1	Mutation	p.E2306X&p.E2327X		
10	66763a0c-6cda-4832-a0cc-e7b496d78eaa	TCGA	NF1	Mutation	p.E2357*		
11	pt_lung_A70	UMICH	NF1	Mutation	p.E540X&p.S749X		
12	e16ca88f-488b-40f0-9169-e5a62482a2ff	TCGA	NF1	Mutation	p.F1357fs	BRAF p.V600E; TP53 p.R196*	
13	bcf2e591-9dae-440f-bd03-5f27c57db741	TCGA	NF1	Mutation	p.G2024*	BRAF p.G469V;	
14	d721bfe0-90e3-415e-b9f3-1a270efa5fbb	TCGA	NF1	Mutation	p.G751*		
15	e10568fe-0436-43f2-9f0f-48f9903868c4	TCGA	NF1	Mutation	p.L1267fs&p.L2538fs		
16	bf15f7ad-9d92-473b-91d1-f24aa373ab97	TCGA	NF1	Mutation	p.L2338H&p.S1938_splice		
17	e487c72f-2cb4-4a88-bd69-cd006d5b4c1a	TCGA	NF1	Mutation	p.I2003_splice		
18	81a0b2ff-a3d3-41bb-9ce6-765e6ae894af	TCGA	NF1	Mutation	p.I396_splice		
19	f462cfef-f60a-4d3e-b92d-b8d8f50b6bb3	TCGA	NF1	Mutation	p.L2413fs	KRAS p.G12C;	
20	7f6455e8-fa3d-4452-acb2-8c9995073072	TCGA	NF1	Mutation	p.L494*&p.E1928fs		
21	c95957a7-1a1a-4c8d-bb61-7c99b500f224	TCGA	NF1	Mutation	p.P1463fs	TP53 p.R158fs; BRAF p.G469V	
22	591c068f-bbb1-4df2-9abb-d1a2e4a58372	TCGA	NF1	Mutation	p.P1951fs		
23	4d687740-96ca-4d78-8c78-1a2024ce6b6c	TCGA	NF1	Mutation	p.Q2492*		
24	46592b7b-6968-42a6-83af-0917c9f4a9a5	TCGA	NF1	Mutation	p.R135fs		
25	ff9def3d-17e5-4ef6-b74e-933f11ed6f00	TCGA	NF1	Mutation	p.R1870_splice	PIK3CA p.N345K; KEAP1 p.P492fs;	
26	bd3bf142-7c14-4538-8a76-3c6e140fa01a	TCGA	NF1	Mutation	p.S2355_splice		
27	42ca54fc-c1ae-41cd-bca1-7fe9810db460	TCGA	NF1	Mutation	p.T1273fs	BRAF p.L514P; TP53 p.V73fs	
28	eeab558b-8d1e-4843-861d-dbf06061758	TCGA	NF1	Mutation	p.T2565fs	EGFR p.L858R	
29	294cb595-0907-44c7-bbef-985a27c1e6e2	TCGA	NF1	Mutation	p.T317fs		
30	8d0736fe-261c-445c-bfd2-a3ea3ceaf367	TCGA	NF1	Mutation	p.W2225*		
31	90b02be3-5496-40a2-8c6e-460d289aadb	TCGA	NF1	Mutation	p.W336*		
32	2e007464-f3f4-4eb2-bab8-91b8272c96d1	TCGA	NF1	Mutation	p.Y2285*		
33	37c8d73a-45ae-40fc-ba9a-721b755c1160	TCGA	NF1	Mutation	p.Y2285fs		

Supplementary Table 8: Lung Cancer Samples Harboring Fusions and/or Outlier Expression of NRG1.

Patient_UUID	Cohort	Disease	Fusion Status	Oncogene Driven	Mutations	Expression Outlier Percentile	NRG1 Expression	Outlier NRG1
							FPKM	Score
pt_lung_A35	UMICH	LUAD	YES	NO	TP53 p.P33R p.P72R; RBM10 p.A630P p.A696P; SMARCA4 p.R513W; APC p.V1822D p.V1804D; ATM p.N1983S	99%	29.08	0.93
ju_lung_lc_s17	SEOUL	LUAD	YES	NO	TP53 p.P33R	99%	33.08	0.93
pt_lung_C028	UMICH	LUAD	NO/TBD	NO	SMARCA4 p.E1056X; TP53 p.R248L p.R209L; APC p.V1822D p.V1804D; ATM p.N1983S	99%	83.92	0.93
0232d299-4cdf-4fd7-9a5e-8d13c208b40c	TCGA	LUAD	NO/TBD	NO	TP53 p.R156P; KEAP1 p.D236N; RBM10 p.S781L	99%	21.32	0.93
7b0622ab-63ea-483f-ae40-d3ea587bdbba	TCGA	LUAD	NO/TBD	NO	-	99%	25.86	0.93
pt_lung_H1793	UMICH	LUAD (LUCL)	NO/TBD	NO	SMARCA4 p.E514X; TP53 p.P33R p.R141H; APC p.V1822D p.E1991D; EGFR p.C311F; ATM p.N1983S	99%	281.86	10.13
a3e1ac67-a1f2-44fb-8343-a7e8239fc24a	TCGA	LUSC	YES	NO	TP53 p.G244C; PIK3CA p.D1045V	99%	49.56	4.23
ce8612ab-3149-4a6a-b424-29c0c21c9b8b	TCGA	LUSC	NO/TBD	NO	TP53 p.S314fs; CDKN2A p.P3fs; APC p.S966G; NF1 p.E1734V	99%	34.53	4.23
7e691df8-8ea6-472c-86bf-504c7ba6983d	TCGA	LUSC	NO/TBD	NO	APC p.S966G; CDKN2A p.P3fs; TP53 p.S314fs; NF1 p.E1734V	99%	49.33	4.23
791f1b21-695e-4db1-b41d-80590c09d257	TCGA	LUSC	NO/TBD	NO	KEAP1 p.R320Q p.R470C; PIK3CA p.E453K	99%	31.24	4.23
14a4a93a-e24d-46f2-bee3-18bd792ef95a	TCGA	LUSC	NO/TBD	NO	TP53 p.E271*	99%	36.74	4.23
6394fe4a-6034-4c79-b28f-aa43e3753730	TCGA	LUSC	NO/TBD	NO	-	99%	57.53	4.23
3351b902-9b7e-4b90-bf6b-bcf74be00bc1	TCGA	LUSC	NO/TBD	NO	-	99%	32.85	4.23
48d-1296-44aa-b7b1-0795939	TCGA	LUSC	Yes	NA	NA	99%	383.00	ND

Supplementary Table 9: Primer Sequences

Primer	5' Gene	3' Gene	Primer ID	Primer Sequence (5'→3')	Length	Product Size
1	AHNAK	KAT5	LF_77F	CTGCCAGACCCGCCCGGAAC	20	152
2	AHNAK	KAT5	LF_77R	AGTCATGCGTGGTGCTGACGG	21	
3	AIM1L	ZNF683	LF_57F	ACCTACAGCGGCACCCAGAGG	21	163
4	AIM1L	ZNF683	LF_57R	GCCCCCTCGCCAGCTCTTTCT	21	
5	ANKRD11	FANCA	LF_53F	GCAGCCCTCGGAGCACGAAT	20	157
6	ANKRD11	FANCA	LF_53R	TGTGCGGCCACCAAAGACCA	20	
7	ATF6B	MUC5B	LF_84F	TGCTCCCAGCCATCAGCCACA	21	110
8	ATF6B	MUC5B	LF_84R	GCCGGCTCGGTCGGTCTTATTG	22	
9	C1ORF194	UQCR10	LF_118F	TACTTAGGAGAACTGCGGGC	20	104
10	C1ORF194	UQCR10	LF_118R	CGGAACAGCAGGGAGTACAA	20	
11	CD74	NRG1	LF_5F	CTGGATGCACCATTGGCTCCTGT	23	110
12	CD74	NRG1	LF_5R	GATGGCTTGTCCCAGTGGTGG	21	
13	CDK9	AHCY	LF_1F	GAACAGCCAGCCCAACCGCTA	21	145
14	CDK9	AHCY	LF_1R	ACGCATCAGGCCCGGCATCT	20	
15	CHST11	TXNRD1	LF_108F	CCAGGACAAAGCCATGAAGC	20	159
16	CHST11	TXNRD1	LF_108R	GCTGGGTTCTCTGGCAAAGT	20	
17	CHST11	TXNRD1	LF_21F	CATCCGCCGCAAGCCTCTCT	20	148
18	CHST11	TXNRD1	LF_21R	ACGGGAGCCTCTGACGACCA	20	
19	COX10	PEMT	LF_100F	CATTGGCTCCGGGCCCTTTTG	21	139
20	COX10	PEMT	LF_100R	CCGAAGGCCCTGCTCAGCTTG	21	
21	CPSF6	TSPAN11	LF_81F	CGCGGATGTCCGGCGAAGAGTTC	22	158
22	CPSF6	TSPAN11	LF_81R	CAGATGCCACAGCCAGGACG	21	
23	CPT1A	HRASLS2	LF_88F	GCACGAGCCCAGACGCCTTT	20	160
24	CPT1A	HRASLS2	LF_88R	GCCGGAGCCAGATGGACCAC	20	
25	CYP24A1	C9ORF3	LF_115F	GTCCGCAAATACGACATCCA	20	193
26	CYP24A1	C9ORF3	LF_115R	GATGTCCAGGGTCAGTTCGAG	21	
27	DAPK1	GMDS	LF_75F	AGCGGAGCTGAAGTGCCCTG	20	152
28	DAPK1	GMDS	LF_75R	CTCCGTCAACGTCCGCAGTGT	21	
29	EIF2AK2	SULT6B1	LF_26F	ACTGCCTAATTCAGGACCTCCACA	24	262
30	EIF2AK2	SULT6B1	LF_26R	CGCACGCATGGCTTGGAAGG	20	
31	ESRP1	DOCK8	LF_76F	CACAGCCTGGCACGGTGGTC	20	192
32	ESRP1	DOCK8	LF_76R	TGCGGGCGTGTCCGGTTTTTC	20	
33	FAM60A	DPF3	LF_19F	TTCCCGGCCAGCGGTAGCAA	20	195
34	FAM60A	DPF3	LF_19R	TCCGGCAGTGCTCAATGGCT	20	
35	FGFR3	TACC3	LF_73F	AGCTACGGGGTGGGCTTCTTCC	22	172
36	FGFR3	TACC3	LF_73R	CGGACGTCCTGAGGGAGTCTCA	22	
37	GTF2E2	GSR	LF_17F	ACACGGCATCAGCGAGGAGA	20	158
38	GTF2E2	GSR	LF_17R	CCCTGCAGCATTTTCATCACACCA	24	
39	HLTF	HPS3	LF_97F	ACGGCCATTGCAGTAATCCTTACCA	25	143
40	HLTF	HPS3	LF_97R	TGGGGCACTTGCTTTGGCTCA	21	
41	IP6K1	TRAIP	LF_3F	GGGAGCAACCTCGGCGCAA	19	145
42	IP6K1	TRAIP	LF_3R	GGCCGGCGGAGCTTCAGATT	20	
43	ITSN1	ENOX1	LF_60F	GGCTCCTGCGTCCCTCCCAG	20	219
44	ITSN1	ENOX1	LF_60R	TGAACATGCGTGGCAGCCTCA	21	
45	JPH1	NCOA2	LF_27F	GGTGGACAGAGCAATTGAAGGCG	23	166
46	JPH1	NCOA2	LF_27R	TCCCATCCCCTCATCTTGAACACA	25	
47	MAPKAPK	ACAD10	LF_83F	GCTCTGCGGCACTGTCACTT	20	256
48	MAPKAPK	ACAD10	LF_83R	ACTGCGAAATCCCACGCCAGG	21	
49	MEAF6	SCMH1	LF_32F	AGGAAGCTGAGCGGCTCTTCAGT	23	196
50	MEAF6	SCMH1	LF_32R	GGCGATGGTGGCTCCTTGTTG	21	

51	MRC2	MAP3K3	LF_15F	GCCTCGTCACCTGCTGCGCT	20	149
52	MRC2	MAP3K3	LF_15R	GACGTCGGTTCATCTGGAGGGC	22	
53	MYO5C	NFAIP8L	LF_55F	GCATCCGTCATGAAGTTACCAGGC	24	177
54	MYO5C	NFAIP8L	LF_55R	GGGCTTGAAGCGCAAGACTCTTTGA	25	
55	NFAT5	VPS4A	LF_37F	AGCGCGGACCTAGACCTGGA	20	100
56	NFAT5	VPS4A	LF_37R	ACTGCACGCACTTGGCTCGAA	21	
57	NFAT5	VPS4A	LF_38F	CAGCGCGGACCTAGACCTGGA	21	155
58	NFAT5	VPS4A	LF_38R	ACTGCACGCACTTGGCTCGAA	21	
59	NUSAP1	EIF2AK4	LF_56F	TGAGTCATCCAAACCTGGAA	20	247
60	NUSAP1	EIF2AK4	LF_56R	TCGCTGAGAAATGACTGCAC	20	
61	PCMT1	LATS1	LF_22F	AGCAACAATCAGTGCTCCACACA	23	139
62	PCMT1	LATS1	LF_22R	TGCTGCAGCCATCTGCTCTCG	21	
63	PPIG	UBR3	LF_79F	GGAGGCGGTTAGCGGGCTTT	20	151
64	PPIG	UBR3	LF_79R	ACGTTGGCAGAAGTCCCAGGC	21	
65	PTCH1	AM120AO	LF_58F	TTTGGGGCCTTCGCGGTGGG	20	112
66	PTCH1	AM120AO	LF_58R	GCCACAGCCTGTCGGTTGCAT	21	
67	PTPRD	LRMP	LF_7F	GCGGCTGCTTTAGTGAAGAAGTGAA	25	160
68	PTPRD	LRMP	LF_7R	ACGCGTTCAACACCATTCTCCA	22	
69	R3HDM2	NFE2	LF_106F	GACTCATGGAGGCTGAGCATT	21	175
70	R3HDM2	NFE2	LF_106R	TCTCCTGCCAAGTCAGTCC	20	
71	R3HDM2	NFE2	LF_107F	CCCTTTTCTTCCCCTCTCC	19	249
72	R3HDM2	NFE2	LF_107R	GGAAAGCCCAGATGGCTCTA	20	
73	R3HDM2	ARHGAP9	LF_123F	CCGCCAAGGCCCGTGCGAG	19	424
74	R3HDM2	ARHGAP9	LF_123R	GCCATCTGCCCCAGTATAAG	20	
75	R3HDM2	ARHGAP9	LF_94F	CTTCCCAAGCCCCTTTCC	18	233
76	R3HDM2	ARHGAP9	LF_94R	ACCGGCTGGATAGCATTGTA	20	
77	RAF1	TMEM40	LF_87F	TGACCCAGTGGTGCGAGGGC	20	152
78	RAF1	TMEM40	LF_87R	TGAGGCTGGGAGGAGGATGCTG	22	
79	RARA	TCAP	LF_113F	TCCTGAATCGAGCTGAGAGG	20	109
80	RARA	TCAP	LF_113R	CAGCTCTGAGGTAGCCATGA	20	
81	RARA	TCAP	LF_114F	ATCGAGCTGAGAGGGCTTCC	20	245
82	RARA	TCAP	LF_114R	GCTGGTGGTAGGTCTCATGTC	21	
83	RARA	TCAP	LF_25F	GCTGAGAGGGCTTCCCCGGTT	21	172
84	RARA	TCAP	LF_25R	GCCCATCCGCATCATCAGCCA	21	
85	RBM12B	MMP16	LF_62F	CCGGCCTTGTGTGCCGACT	20	254
86	RBM12B	MMP16	LF_62R	GAGCGGTGTGGGGGCACTGT	20	
87	RUNX1	PTPRR	LF_13F	GCTGAGAAATGCTACCGCAGCCA	23	144
88	RUNX1	PTPRR	LF_13R	ACCGGCTTCCCACTCTTCTTCTGA	24	
89	SLC12A7	TERT	LF_2F	GCCTACGCCAGACAAGGTGCAG	22	159
90	SLC12A7	TERT	LF_2R	TCTGCTTCCGACAGCTCCCCG	21	
91	SLC37A1	TIAM1	LF_122F	CTCGGCAACTGGTTTGAA	19	286
92	SLC37A1	TIAM1	LF_122R	ACCATATGACCGTCAGGCTTC	21	
93	SLC37A1	TIAM1	LF_82F	GGGGCCTGTCCTTCGTCGTG	20	125
94	SLC37A1	TIAM1	LF_82R	GCGACCATCAACCGTCACCAGG	22	
95	SLC9A7	VDR	LF_4F	GCTCACGCTCACCATCTCACC	22	160
96	SLC9A7	VDR	LF_4R	AGCAGGGGGCAGGTAAGTGGA	21	
97	SMARCB1	BCL2L13	LF_67F	TGGGCAGAAGCTGCGAGACG	20	137
98	SMARCB1	BCL2L13	LF_67R	CCTGGAACACACAGCGCCTGG	21	
99	SRGAP1	MSRB3	LF_20F	AGCAAAGACCATGCAACCTTGAGT	24	123
100	SRGAP1	MSRB3	LF_20R	ACGAGAAGCAAAGAACAGGGGCA	23	

101	SRSF7	SOS1	LF_34F	ACCTGCCCGACGTCCCTTG	20	156
102	SRSF7	SOS1	LF_34R	GGACCTCAGGGTTGCCTTCTTCTG	24	
103	TFG	GPR128	LF_78F	TGCAACGAGTTTTTCAGAGGA	20	231
104	TFG	GPR128	LF_78R	GTAGGGGTGCTTGATGAGGA	20	
105	THADA	MTA3	LF_43F	TGGGAGTCAGCCAGGAAGGTGT	22	176
106	THADA	MTA3	LF_43R	GCTTCAGAGGCTGACCATTCTCC	24	
107	TMEM131	HRHGAPI3	LF_121F	TCACGAAATGCCAGAAAACA	21	206
108	TMEM131	HRHGAPI3	LF_121R	ACTTTGTGCAGATGAGAGCCA	21	
109	TMEM131	HRHGAPI3	LF_80F	GGCAACACCAGTAGCTCAGAGGG	23	95
110	TMEM131	HRHGAPI3	LF_80R	TGCAGTCTGAACAAGCTGCCAGG	23	
111	TNFRSF14	IGHM	LF_102F	CTGACCCACAGACTCTGCAC	20	252
112	TNFRSF14	IGHM	LF_102R	GGGAATTCTCACAGGAGACG	20	
113	TP53	SAT2	LF_24F	GGCTCCGGGGACACTTTGCG	20	121
114	TP53	SAT2	LF_24R	GCCAGCGAGGCGATCCTCTG	20	
115	TP53	GLP2R	LF_31F	TTTGCCTTCGGGCTGGGAGC	20	149
116	TP53	GLP2R	LF_31R	TGGCGGGCTAGCAAGAAGCG	20	
117	TSC1	SMARCA4	LF_30F	AAGCCAATGATGGAGCATGTGCG	23	121
118	TSC1	SMARCA4	LF_30R	ACCTTCACCGGGAGGTCGCT	20	
119	TTC1	DOCK2	LF_101F	AGGAGGAGCCAGGAGCGGAC	20	177
120	TTC1	DOCK2	LF_101R	AGTAGTGCTGGTCACCCATCTGGT	24	
121	UBA5	MRAS	LF_99F	TTGCAGGAAGCAGCAGGAGGAA	22	151
122	UBA5	MRAS	LF_99R	TTGTCACTGGGGACGGCGCT	20	
123	WASF2	FGR	LF_11F	CGGGAGCACACTCTGTGCGGA	21	108
124	WASF2	FGR	LF_11R	GCTGCGGCATGATCCTTGGA	21	
125	ZNF544	ZNF17	LF_46F	CACCAGGCAGGTGACGCCTA	20	189
126	ZNF544	ZNF17	LF_46R	ACATTGCTTGGAAGGTGCCTCCTC	24	
127	ZNF664	WSB2	LF_47F	CGCCGGACGCCTCCATTGTT	20	181
128	ZNF664	WSB2	LF_47R	CCGGGCTTGAGTTCGGCCAG	20	
129	ZNF667	DC1001282	LF_69F	CGGAACCTGGTCTCGCTTGGT	21	150
130	ZNF667	DC1001282	LF_69R	GCTCTCCTGCGATCATTCCGCA	22	
131	ZNF704	MYC	LF_14F	CCAGACGACGGCATCGACGAG	21	151
132	ZNF704	MYC	LF_14R	ACGGCTGCACCGAGTCGTAG	20	
133	ZSWIM4	RFX1	LF_28F	CCTGAGCCCCCACTGCAAACC	21	174
134	ZSWIM4	RFX1	LF_28R	ACTGTCTCGCTGGCCCCGCAT	20	
135	GAPDH			CTCTGCTCCTCCTGTTTCGAC	20	112
136	GAPDH			ACGACCAAATCCGTTGACTC	20	
137	ACTB F			CTCTTCCAGCCTTCCTTCT	20	116
138	ACTB R			AGCACTGTGTTGGCGTACAG	20	

Supplementary Data 1: Clinicopathological Characteristics of the Combined Lung Cohort Used in this Study.

Supplementary Data 2: Fusions Recovered by the Classifier in the ju_lung Cohort.

Supplementary Data 3: Fusions Recovered by the Classifier in UMICH Cohort.

Supplementary Data 4: Lung Fusions Candidates after Classification.

Supplementary Data 5: Table with Recurrence of Known Fusions across the Full Cohort and in Samples with Unknown Drivers.

Supplementary Data 6: Fusions found in the HIPPO Pathway in NSCLC.

Supplementary Data 7: Differentially expressed genes in BEAS-2B cells expressing CD74-NRG1 fusion protein versus LacZ.

Supplementary Data 8: Fusions Used as True Positives for the Random Forest Classifier.

Supplementary Data 9: List of gene fusions identified by TOPHAT analysis in normal samples

Supplementary Methods:

Bioinformatics Methods

Sequence Alignment

Sequence alignment was performed using the Tuxedo pipeline: Bowtie2 (Bowtie2/2.0.2) and Tophat2 (TopHat/2.0.6)^{1, 2}. We supplied TopHat with the set of transcript models annotated in the *Homo sapiens* ensemble database version 69. The flag fr-firststrand was used for the strand specific RNASeq libraries while fr-unstranded was used for the unstranded libraries. All other parameters were used with default values.

Fusion Calling

Fusion calling was performed with TopHat-fusion1 (THF) on the UMICH, TCGA and SEOUL cohorts. TopHat-fusion was run with the following arguments: bowtie1, fusion-search, keep-fastq-order, no-coverage-search, fusion-min-dist=0, fusion-anchor-length=13, fusion-ignore-chromosomes=chrM. TopHat post-processing was run with the arguments: skip-blast, num-fusion-reads=1, num-fusion-pairs=1, num-fusion-both=3.

Fusion Annotation and Lung Cancer Fusion Database

A database of fusions in lung cancers was developed, and for each fusion structural and functional annotation was recorded. The structural information correspond to chromosome number of 3' and 5' partner genes, cohort, 3' and 5' chromosome location, 3' breaking exon, 5' breaking exons, median alignment quality of reads that support 3' gene, median alignment quality of reads that support 5' gene, number of spanning reads, spanning mate pairs and encompassing reads, 3' and 5' partner recurrence across the cohort and fusion type (Inter-chromosomal, Intra-chromosomal, Tandem-duplication).

The functional annotation corresponds to kinase status, oncogene status, tumor suppressor status and targetable status (TRUE/FALSE) of both 3' and 5' partner genes. Other functional annotations include the gene family of both fusion genes, as well as the gene biotype (protein-coding, ncRNA, rRNA, etc.). Moreover, the gene expression of each fusion gene was calculated in fragments per-kilobase per million (FPKM) using Cufflinks3 and stored in the database. In addition, an outlier score was calculated for the expression of both 5' and 3' partners in order to identify cases in which the 3' partner is highly expressed as consequence of the fusion event.

This database was created using pytables and hd5 format for fast access and storage and includes the following tables: patient table, patient clinical information table, fusions structural information table and expression table. In addition to these tables corresponding to fusion events, we create an additional table to store the mutation status for each patient, mutation table. The mutation table allows us to classify each patient as

“driver positive” or “driver negative” according to mutation status of well-known cancer related genes (see below).

Mutation Calling

UMICH cohort: Single nucleotide variants (SNVs) were called using VarScan2 (VarScan2/2.2.8)³ on the ssRNAseq libraries of the UMICH cohort. Because, we did not have matched normal for each tumor sample, we consider only SNVs that were previously reported in the Catalogue of Somatic Mutations database (COSMIC version 56). Single nucleotide mutations in other positions were not considered for reporting or downstream analysis. SNVs present in dbSNP (v135) were filtered out, as well as SNVs with variant fraction smaller than 10%, or with less than six reads covering the position. Insertions and deletions were not called from the RNAseq data, because currently there are no available algorithms to efficiently assess these genetic aberrations on RNASeq libraries. SNVs for all tumor samples were aggregated and annotated using variant-tools⁴. TCGA cohort: All somatic mutations both SNVs and indels called on Exome sequencing data for the TCGA consortium were extracted from aggregated Mutation Annotation Format (MAF) files available at the Broad institute firehose Genome Data Analysis Center MAF dashboard on May 11 of 2013. SEOUL cohort: All SNV and insertion/deletion somatic mutations reported by Seo et al (2012) were used⁵.

Sample Annotation

We annotated the mutation status of well characterized oncogenes and tumor suppressors known to be involved in lung adenocarcinoma and squamous carcinoma. We considered activating mutations for *KRAS*, *NRAS*, *HRAS*, *EGFR*, *BRAF*, *PIK3CA*, *MET*, and missense or non-sense mutations for *TP53*, *STK11*, *NF1*, *PTEN*, *SMARCA4*, *CDKN2A*, and *APC* genes. Mutations reported in COSMIC were considered for *AKT*, *MEK*, *ATM*, *AKT1*, *KEAP1*, *U2AF1*, *RBM10*, *ARID10*, and *MYC* which have been recently implicated on these indications^{6, 7}. Finally, we used the somatic mutation information to divide the combined cohort in two groups: samples with known drivers and samples of unknown drivers. The first group corresponds to samples with somatic mutations in *KRAS*, *NRAS*, *HRAS*, *EGFR*, *BRAF* and/or *PIK3CA*, while the second group to samples that do not harbor alterations in those well-known driver genes.

Fusions Classifier Training

First, all fusions present in normal samples were considered false positives and filtered out **Supplementary Data 9**. For the classification step, we trained a random forest classifier with 10000 trees using the following features: chromosomes of 3' and 5' genes, 3' gene, 5' gene, 3' breaking exon, 5' breaking exons, median alignment quality of reads that support 3' gene, median alignment quality of reads that support 5' gene, number of spanning reads, spanning mate pairs and encompassing reads, 3' and 5' partner recurrence, fusion type, gene biotype of both 3' and 5' genes, FPKM expression of both 3' and 5' genes, and FPKM expression of both 3' and 5' genes normalized across the combined cohort.

Experimental Methods

RNASeq Library Preparation

Transcriptome libraries were prepared following a modified protocol previously described for generating strand specific RNASeq libraries⁸. Briefly 2.5 µg of total RNA was subjected to polyA selection using oligodT beads (Invitrogen, Carlsbad, CA). Purified polyA RNA was fragmented and reverse transcribed using Superscript-II (Invitrogen, Carlsbad CA). Second strand synthesis was performed with DNA Polymerase I (New England Biolabs, Ipswich, MA) in the presence of dNTP mix containing dUTP instead of dTTP. The product was then subjected to end repair, A base addition and adaptor ligation steps. Libraries were next size selected in the range of 350 bps after resolving in a 3% Nusieve 3:1 (Lonza, Basel, Switzerland) agarose gel and DNA recovered using QIAEX II gel extraction reagent (Qiagen, Valencia, CA). Libraries were barcoded during the 14-cycle PCR amplification with Phusion DNA polymerase (New England Biolabs, Ipswich, MA) and purified using AMPure XP beads (Beckman Coulter, Brea, CA).

Quantitative RT-PCR and PCR Fusion Validation

Complimentary DNA was synthesized from total RNA using Superscript III in presence of random primers (Invitrogen, Carlsbad, CA). Quantitative Real-time PCR (qPCR) was performed using SYBR Green Master mix on the StepOne Real-Time PCR System (Applied Biosystems). All oligonucleotide primers for the qPCR assays were obtained from Integrated DNA Technologies (Coralville, IA); *NRG1* forward 5'GATTCCTACCGAGACTCTCCTC3' and reverse 5'TGGAAGGCATGGACACCGTCAT3' and *GAPDH* forward 5'GTCTCCTCTGACTTCAACAGCG3' and reverse primer 5'ACCACCCTGTTGCTGTAGCCAA3'. Fold changes were calculated relative to *GAPDH* and normalized to the non-target control sample.

We validated a subset of nominated fusion genes by THF from UMICH cohort using real-time RT-PCR. Subsequently the products were resolved in a 2% agarose gel electrophoresis for size evaluation. Of the 29 attempted fusions, 28 were validated, representing a validation rate of 96.6% (**Supplementary Data 4**). The primer sequences for PCR fusion validation and PCR product sizes are listed in **Supplementary Table 9**.

siRNA knockdown studies

Lung cancer cell line NCI-H1793 were plated in 6-well plates at a desired numbers and transfected with 2nmol of *NRG1* siRNAs (J-004608-11; and J-004608-12) or non-target control siRNA (Thermo Scientific). Transfection with Oligofectamine reagent (Invitrogen, Carlsbad, CA) was performed twice over a period of 48 hours. Knockdown efficiency was determined by qPCR. For cell proliferation assay 24 hours after transfection, cells were trypsinized and plated in triplicate at 8,000 cells per well in 24-well plates. The plates were incubated in the IncuCyte live-cell imaging system

(Essen Biosciences) at 37°C under 5% CO₂ atmosphere. Cell proliferation rate was assessed by kinetic imaging confluence measurements at 3-hour time intervals.

Protein Isolation and Western Blot Analysis

Cells were washed with ice cold PBS twice and harvested using cell lysis buffer (Cell Signaling). Protein concentrations were estimated (bicinchoninic protein assay, Pierce, Rockford, IL) and equal amounts were resolved under reducing conditions by 10% SDS-PAGE. The protein was transferred to PDVF membranes, blocked in 5% milk tris-buffered saline (TBS) containing 0.1% Tween 20 and incubated with respective antibodies against for overnight at 4°C. The membrane were washed three times with 0.1% Tween 20 - TBS and further incubated for 60 minutes with secondary HRP anti-rabbit IgG used at 1:2000 dilution. Antibodies against E-Cadherin, Vimentin, phospho-ErbB3, phospho-ErbB3, phospho-ERK and total-ERK were purchased from Cell Signaling Technology Inc. (Beverly, MA). Total ErbB3 and ErbB4 were purchased from Santa Cruz Biotechnology Inc. (Dallas, TX). The membrane-bound peroxidase activity was detected using ECL Prime Western Blotting Detection kits (Amersham, Arlington Heights, IL) and the chemiluminescence signal were captured by exposing to autoradiographic films.

Supplementary References:

1. Kim D, Pertea G, Trapnell C, Pimentel H, Kelley R, Salzberg SL. TopHat2: accurate alignment of transcriptomes in the presence of insertions, deletions and gene fusions. *Genome Biology* **14**, R36 (2013).
2. Trapnell C, *et al.* Differential gene and transcript expression analysis of RNA-seq experiments with TopHat and Cufflinks. *Nature Protocols* **7**, 562-578 (2012).
3. Koboldt DC, *et al.* VarScan 2: somatic mutation and copy number alteration discovery in cancer by exome sequencing. *Genome Research* **22**, 568-576 (2012).
4. San Lucas FA, Wang G, Scheet P, Peng B. Integrated annotation and analysis of genetic variants from next-generation sequencing studies with variant tools. *Bioinformatics* **28**, 421-422 (2012).
5. Seo JS, *et al.* The transcriptional landscape and mutational profile of lung adenocarcinoma. *Genome Research* **22**, 2109-2119 (2012).
6. Comprehensive genomic characterization of squamous cell lung cancers. *Nature* **489**, 519-525 (2012).
7. Weir BA, *et al.* Characterizing the cancer genome in lung adenocarcinoma. *Nature* **450**, 893-898 (2007).
8. Levin JZ, *et al.* Comprehensive comparative analysis of strand-specific RNA sequencing methods. *Nature Methods* **7**, 709-715 (2010).

